Biomass Accumulation and Clogging in Biotrickling Filters for Waste Gas Treatment. Evaluation of a Dynamic Model Using Dichloromethane as a Model Pollutant

W. J. H. Okkerse,[1] S. P. P. Ottengraf,[1,2] B. Osinga-Kuipers,[1] M. Okkerse[1]

[1]Eindhoven University of Technology, P.O. Box 513, STW 0.35, 5600 MB, The Netherlands; telephone: +31 40 2473669; fax: +31 40 2439303; e-mail: tgtcwo@chem.tue.nl
[2]University of Amsterdam, Nieuwe Achtergracht 166, 1018 WV Amsterdam

Received 9 May 1998; accepted 8 November 1998

Abstract: A dynamic model is developed that describes the degradation of volatile acidifying pollutants in biotrickling filters (BTFs) for waste gas purification. Dynamic modelling enables the engineer to predict the clogging rate of a filter bed and the time it takes the BTF to adapt to changes in its inlet concentration. The most important mechanisms that govern the behaviour of the BTF are incorporated in the model. The time scale of the accumulation of biomass in a filter is investigated, and an approach is presented that can be used to estimate how long a BTF can be operated before its packing has to be cleaned. A three-month experiment was carried out to validate the model, using dichloromethane (DCM) as a model acidifying pollutant. Valuable experimental data about biomass accumulation and liquid hold-up in the reactor were obtained with an experimental set-up that allows the continuous registration of the weight of the BTF. The results show that in BTFs eliminating DCM from a waste gas, clogging is not to be expected up to concentrations of several g/m^3. Model calculations based on the measurements also suggest that the maximum carbon load that can safely be applied per unit void packing volume should not exceed 0.5–1.6 C mol/(m^3 · h), depending on the density of the biofilm formed. The model is a good predictor of the elimination of the pollutant in the system, the axial gas and liquid concentration profiles, the axial biomass distribution, and the response of the system upon a stepwise increase in the DCM inlet concentration. The influence of the buffer concentrations in the liquid phase upon the performance of the BTF is investigated. *Biotechnol Bioeng* **63**: 418–430, 1999.
Keywords: waste gas treatment; biological trickling filters; biofilm; dichloromethane; biofiltration; air pollution control; dynamic model

INTRODUCTION

Biotrickling filters (BTFs) can successfully be applied to remove volatile pollutants from waste gases. The waste gas is forced through a packed column that is continuously wetted by a recycled water phase. Micro-organisms are present in a biofilm that develops on the packing material after inoculation with a suitable bacterial suspension. The target compound and oxygen are transferred from the gas phase into the biofilm, where microbiological degradation occurs. The temperature, pH, ionic strength, and nutrient level of the recycled water can be maintained at a desired setting. Therefore, BTFs are especially suitable for the treatment of waste gases that contain acidifying compounds. These are compounds that stoichiometrically liberate strong acids when they are biologically oxidised, e.g., chlorinated hydrocarbons, organo-sulphur compounds, hydrogen sulphide, and ammonia (Diks, 1992). A further beneficial feature of BTFs is that their inert packing material can be cleaned by regular backwashing, or by removing and cleaning packing elements in moving bed type of reactors. This makes the treatment of fairly concentrated waste gases possible that otherwise would lead to clogging of the reactor within a short time (Alonso et al., 1997; Weber, 1995). Several steady-state models have been proposed to describe the elimination of volatile pollutants under different gas- and liquid-loading rates, and some analytical solutions are available (Diks and Ottengraf, 1991; Hekmat and Vortmeyer, 1994). These models are suitable for quick design purposes and provide insight into the dominating BTF phenomena in the steady state.

In industry, a filter usually experiences fluctuating inlet concentrations. Moreover, excessive biomass accumulation, an intrinsically time-dependent process, is observed at higher volatile organic compound (VOC) inlet concentrations. These phenomena cannot be described by steady-state models, and for optimisation purposes dynamic models have to be applied. In the last half decade, several dynamic biofilter models have been proposed. They describe the influence of a change in the inlet concentration on the removal

Correspondence to: W. J. H. Okkerse

 CCC 0006-3592/99/040418-13

efficiency of the biofilter. Biomass growth is usually not considered and a constant biofilm thickness is assumed (Deshusses, 1995; Shareefdeen and Baltzis, 1995; Zarook et al., 1997).

A dynamic BTF model has been presented by Alonso et al. (1997) that includes biomass growth and a variable biofilm thickness along the column. The authors also account for a decreasing mass transfer coefficient in their system due to excessive biofilm formation upon the packing. Deactivation of biomass was neglected, as the assumption was made that all biomass in the column is viable. However, in systems with an extended retention time, this assumption is not valid, since a major part of the cells is inactive (Bryers and Mason, 1987). Furthermore, only diffusion limitation of the pollutant was taken into account, while it is known that oxygen can become the rate-limiting substrate at higher VOC inlet concentrations (Deshusses et al., 1995; Diks, 1992; Kirchner et al., 1996; Shareefdeen, 1993).

In the model presented here, a distinction is made between active and inactive biomass, which makes it possible to describe the long term BTF behaviour. Because the degradation of acidifying compounds is studied, it is necessary to consider reaction inhibition by acidification of the liquid phase. Due to recirculation of the liquid phase no equilibrium exists between gas and liquid phase concentrations as presumed in the model by Alonso et al. (1997), and a different approach is taken here.

The purpose of the present study is to discuss some model predictions relevant to the field of biological waste gas treatment and to study in more detail the dynamics of the degradation of dichloromethane (DCM), as well as the biomass accumulation in a BTF. It is furthermore the intention to estimate a maximum allowable carbon load that can be imposed on a filter.

THEORY

The dynamic BTF model is based upon the calculation of transversal biofilm concentration profiles and axial gas and liquid concentration profiles in the column. Substrate degradation and progression of the biofilm thickness are modelled according to Wanner and Gujer (1986). This type of model has been investigated intensively in biofilm research for waste water treatment systems, both theoretically and in laboratory set-ups (Horn and Hempel, 1997; Rittmann and Hanem, 1992; Wik and Breitholtz, 1996). The pseudo steady state that establishes itself after some time of operation was studied by Skowlund (1990). Gas-to-biofilm mass transfer is modelled using the approach of Diks and Ottengraf (1991). Acid is liberated during the oxidation process of DCM causing the pH to decrease. To describe the inhibitory effect of acidification, an electroneutrality or alkalinity balance has been incorporated in the model to calculate the pH gradient inside the biofilm and along the column.

The combined model describes the concentration profiles of the substrate and metabolites in the biofilm, as well as the axial gas and liquid bulk concentrations. Furthermore, it gives the biofilm development in time. A scheme of the reactions taken into account is given in Fig. 1, and the accompanying model are given by Eqs. (1)–(15).

The volumetric rate of reaction of DCM, r_{DCM}, is described by a double Monod equation and a correction term F_{pH} that describes the pH dependence of the reaction (Eq. (1)). A single type of viable species is taken into account. Its biomass is subject to decay (Eq. (3)), where a fraction Y_{inert} of the biomass is converted into inert solid material (Eq. (4b)), e.g., cell debris, extracellular polymers, etc. The rate of biomass mineralisation or rate of decay (r_d) is assumed to be of first order with regard to the active biomass concentration X_{act}, while a Monod type dependency with regard to the oxygen concentration in the biofilm is assumed (Eq. (3)). Oxygen, DCM, inorganic carbon species, and chloride are the four diffusing reactants considered in the biofilm (Eq. (9)). The last term on the right-hand side of this equation accounts for the velocity u_L, which is the biofilm–water interface expansion rate in the transversal direction. The volume fractions of active DCM degrading biomass f_{act} and inerts f_{inert} are a function of the position in the biofilm and of time. The change in time of these fractions at various positions in the biofilm is described by a mass balance (Eq. (12)).

Intrinsic rate equations

Substrate consumption: $r_{DCM} =$

$$-F_{pH} \cdot \mu_{max} \cdot X_{act} \cdot \frac{1}{Y_{DCM}} \cdot \frac{S_{DCM}}{S_{DCM} + K_{DCM}} \cdot \frac{S_{O_2}}{S_{O_2} + K_{O_2}} \quad (1)$$

pH correction factor: $F_{pH} = \exp\left[-A(\mathrm{pH} - B)^2\right]$ (2)

Biomass decay: $r_d = k_d \cdot X_{act} \cdot \frac{S_{O_2}}{S_{O_2} + K_{O_2}}$ (3)

Specific production of active DCM degrading biomass:

$$\mu_{act} = -\frac{r_{DCM}}{X_{act}} \cdot Y_{DCM} - \frac{r_d}{X_{act}} \quad (4a)$$

of inerts: $\mu_{inert} = \frac{r_d}{X_{inert}} \cdot Y_{inert}$ (4b)

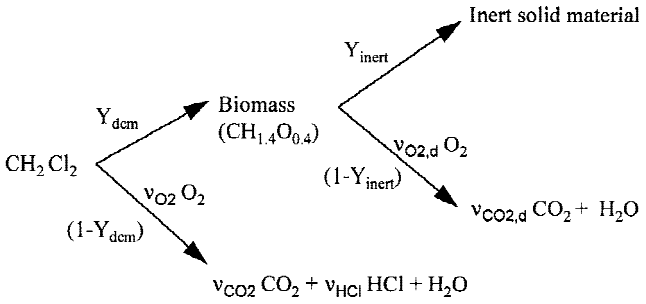

Figure 1. The degradation reactions considered in the dynamic mathematical model.

Buffers for calculation of the axial and transversal pH gradient

$$\frac{c_{L,H^+}}{M_{H^+}}+\frac{c_{L,K^+}}{M_{L,K^+}}+\frac{c_{L,Na^+}}{M_{L,Na^+}}=\frac{c_{L,Cl^-}}{M_{L,Cl^-}}+2\cdot\frac{c_{L,HPO_4^{2-}}}{M_{L,HPO_4^{2-}}}+\frac{c_{L,H_2PO_4^-}}{M_{L,H_2PO_4^-}}+\frac{c_{L,HCO_3^-}}{M_{L,HCO_3^-}} \quad (5a)$$

$$K_1=\frac{c_{L,H^+}/M_{H^+}\cdot c_{L,HPO_4^{2-}}/M_{L,HPO_4^{2-}}}{c_{L,H_2PO_4^-}/M_{L,H_2PO_4^-}};\qquad K_2=\frac{c_{L,H^+}/M_{L,H^+}\cdot c_{L,HCO_3^-}/M_{L,HCO_3^-}}{c_{L,CO_{2,aq}}/M_{L,CO_{2,aq}}} \quad (5b)$$

$$P_t=c_{L,iH_2PO_4^-}/M_{H_2PO_4^-}+c_{L,iHPO_4^{2-}}/M_{HPO_4^{2-}}\text{ and}\qquad C_t=c_{L,iHCO_2^-}/M_{HCO_2^-}+c_{L,iCO_{2,aq}}/M_{CO_{2,aq}} \quad (5c)$$

Stoichiometric relationships

$$r_{0_2}=\upsilon_{O_2}r_{DCM}-\upsilon_{O_2,d}r_d \quad (6)$$

$$r_{HCl}=-\upsilon_{HCl}\cdot r_{DCM} \quad (7)$$

$$r_{CO_2}=\upsilon_{CO_2,d}r_d-\upsilon_{CO_2}r_{DCM} \quad (8)$$

Dimensionless unsteady-state reaction/diffusion equations in the planar biofilm

$$\frac{\partial S_i}{\partial t}=r_i+\frac{1}{L^2}\frac{\partial\Gamma_i}{\partial\zeta}+\frac{\zeta\cdot\mu_L}{L}\frac{\partial S_i}{\partial\zeta},\quad \zeta=\frac{x}{L},\quad \Gamma_i=D_i\frac{\partial S_i}{\partial\zeta}, \quad (9)$$

with boundary conditions $\zeta = 1$, $S_i = c_{L,i}$, and $\zeta = 0$, $\frac{\partial S_i}{\partial\zeta}=0$ and initial conditions t = 0, $L = L_0$.

Biofilm expansion

Definition of active/inactive fraction:

$$f_{act}=X_{act}/X,\ f_{inert}=X_{inert}/X\quad\text{with } X_{act}+X_{inert}=X \quad (10)$$

Average local growth rate: $\bar{\mu}=\mu_{act}\cdot f_{act}+\mu_{inert}\cdot f_{inert}$ (11)

Change in local fraction:

$$\frac{\partial f_{act}}{\partial t}=(\mu_{act}-\bar{\mu})\cdot f_{act}-\frac{(\mu-\zeta\cdot\mu_L)}{L}\frac{\partial f_{act}}{\partial\zeta} \quad (12)$$

Biofilm rate of expansion: $u=L\cdot\int_0^\zeta\bar{\mu}\,d\zeta$, (13)

with boundary conditions at $t = 0$, $f_{act} = 1$.

Macrobalances reactor

$$\text{Gas: }\frac{dc_{G,DCM}}{d\sigma}=\pm\frac{H\cdot k_{og}a_w}{\nu_g}(c_{G,DCM}-m\cdot c_{L,DCM});\quad +\text{ cocurrent, }-\text{ countercurrent} \quad (14)$$

$$\text{Liquid: }\frac{dc_{L,DCM}}{d\sigma}=-\frac{H\cdot k_{og}a_w}{\nu_L}(c_{G,DCM}-m\cdot c_{L,DCM})+\frac{H\cdot\Gamma_{DCM,L}\cdot a_w}{\nu_L};\ \sigma=z/H, \quad (15)$$

with boundary conditions $c_{L,DCM}(\sigma = 0) = c_{L,DCM}(\sigma = 1)$; cocurrent, $\sigma = 1$, $c_{g,DCM} = C_{g,0}$ and countercurrent, $\sigma = 0$, $c_{g,DCM} = C_{g,0}$.

The experiments showed that biofilm loss through shear is negligible during the time period considered in the present study. The velocity u_L is then given by the integral of the average growth rate over the entire length of the biofilm described by Eq. (13) (Wanner and Gujer, 1986).

It is assumed that the pH profile is determined by the diffusion of counter-ions of protons (e.g., chloride and carbonate species). With this assumption, the proton concentration can be calculated via the requirement of local electroneutrality in the biofilm (Eq. (5a)), using the sodium, potassium, and total phosphate concentrations given (Liou and Rousseau, 1986; Szwerinski et al., 1986). The local Cl^- and total carbonate concentration were obtained from the reaction–diffusion equation (Eq. (9)). The concentrations of the phosphate and carbonate ions are obtained by the assumption of local equilibrium of the dissociation reactions (Eq. (5b)). Other dissociation reactions are not considered as they are only of minor importance in the pH range considered. Although it is known that biomass generally possesses pH buffering properties, this effect does not play an important part due to the assumed pseudo steady-state concentration profiles of substrate and products in the biofilm.

Liquid and gas phase macrobalances were set up for the substrate DCM (Eqs. (14) and (15)). Besides a DCM liquid phase balance, also a balance for the chloride ions had to be made to obtain a pH profile over the column height. As a first approximation, the O_2 and CO_2 concentration in the bulk liquid are assumed to be in equilibrium with the concentration in the inlet air and exit air respectively. Eq. (15) also holds for nonvolatile reactants, e.g., Cl^-, omitting the gas/liquid transport term. The DCM elimination capacity (EC) is calculated from the difference between the inlet and exit gas phase concentration. The rate of CO_2 production in the filter (R_{CO2}) is obtained from the carbonate concentration profiles at the biofilm–water interface (Eq. (9)) by calculating the total flux through the biofilm–water interface present in the reactor. The static hold-up G_{stat} is obtained by integration of the biofilm thickness L along the height of the BTF.

MODEL PARAMETERS

Model parameters were either obtained from literature or experimentally determined in this study. Table I contains the values of the parameters used in the simulations and their source.

The mass transfer coefficient of a plastic packing material increases considerably when it becomes grown by a biofilm

Table I. Parameter values used in the model simulations.

μ_{max} [a]	2.2×10^{-5}	(l/s)	K_2	7.7×10^{-7}	(mol/dm^3)
A [b]	0.2	(–)	K_{O2} [h]	0.1×10^{-3}	(kg/m^3)
B [b]	7.6	(–)	K_{DCM} [a]	0.9×10^{-3}	(kg/m^3)
ν_{HCl}	2	(–)	m [c]	0.09	(–)
ν_{CO2}	0.53	(–)	$k_{og}a_w$ [c]	0.067	(l/s)
$\nu_{CO2,d}$	1.0	(–)	a_w [i]	135	(m^2/m^3)
ν_{O2}	0.46	(–)	H	2.7	(m)
$\nu_{O2,d}$	1.15	(–)	V_r	0.33	(m^3)
Y_{DCM} [d]	0.47	(mol/mol)	v_g	7.3	(m/h)
D_{DCM} [b]	0.31×10^{-9}	(m^2/s)	v_l	163	(m/h)
D_{HCO3-} [e]	0.30×10^{-9}	(m^2/s)			
D_{Cl-} [f]	0.44×10^{-9}	(m^2/s)			
D_{O2} [f]	0.51×10^{-9}	(m^2/s)	Initial conditions		
ρ_b [c]	1090	(kg/m^3)	$f_{act,0}$	1	(–)
K_l [g]	6.2×10^{-8}	(mol/dm^3)	L_0	8.0	(μm)

[a]Diks (1992): Table 3-III, TF-Enrichment culture.
[b]Derived from Fig. 2.14 (Diks, 1992).
[c]This study.
[d]Roels (1983).
[e]Szwerinski et al. (1986).
[f]Janssen and Warmoeskerken (1979).
[g]Corrected for the salt concentration. Mehrbach et al. (1973).
[h]Wanner and Gujer (1986).
[i]Okkerse and Ottengraf (1997).

(Okkerse and Ottengraf, 1997; Pedersen and Arvin, 1997). In the present study, the overall gas–liquid mass transfer coefficient was determined by the inert tracer experiments described in the materials and methods section. The specific area of the packing that is available for growth is assumed to be equal to the wetted packing area a_w. The latter was determined in a previous study by measuring the absorption of CO_2 in caustic soda (Okkerse and Ottengraf, 1997). Diffusion coefficients are set according to the equation given by Fan et al. (1990), using a dry biofilm concentration of 90 kg/m^3 as measured by Diks (1992).

MATERIALS AND METHODS

Biological Trickling Filter

The experimental set-up is shown in Fig. 2. The same set-up was used in a previous study (Diks and Ottengraf, 1991). The column was made of glass fibre enforced plastic (4 m high, 0.396 m inner diameter) and was equipped with a liquid distributor, temperature and pH control units, DCM dosing system, and feed and drainage appendages. A few modifications were made: an arranged instead of a dumped packing material was used and the total column was freely suspended from a load cell (Z6H3, Hottinger Baldwin Messtechnik, Darmstadt, Germany). The total height of the packing was 2.7 m divided into 3 stages with a 10 cm spacing between the stages to facilitate sampling and to provide room for liquid redistributors. Each stage consisted

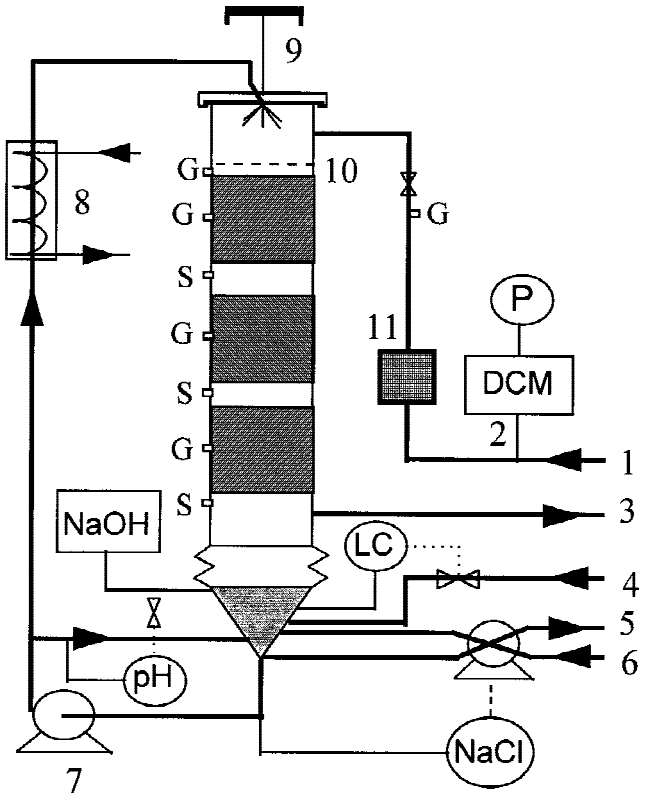

Figure 2. Biotrickling filter set-up. S, liquid/gas sampling port; G, gas sampling port; 1, gas inlet; 2, DCM addition; 3, purified waste gas outlet; 4, level control and tap water supply; 5, drain; 6, nutrient feed; 7, recycle pump; 8, temperature control; 9, load cell; 10, liquid distributor; 11, static gas mixer.

of three packing elements of 30 cm giving a total height of 2.7 m of packing. A tight fit existed between the packing and the wall of the column. A corrugated sheet 60° PVC cross-flow cooling packing was used with a specific surface of 240 m^2/m^3 and a voidage of 97% (c10.12, ME Aachen, Aachen, Germany). All pipes and hoses were attached in such a way that they applied a negligible vertical force to the column. This made a stable and continuous registration possible of the total mass of the column with the load cell. During standard operation a data point was automatically sampled every 10 min. The error of the signal was less than 3% with a lower limit of about 50 g. A hold-up curve was made by stopping the liquid flow and recording the BTF's mass during the course of time using a data acquisition system. The artificial waste gas was made by dosing liquid DCM into an ambient air stream. When quantitative measurements were carried out, an accurate peristaltic syringe pump (LC2600, Isco Inc., Lincoln, NE) was used to dose the liquid DCM into the gas stream. Mixing was facilitated by a 20 dm^3 static gas mixer placed after the liquid DCM addition and stable concentrations up to 12 g DCM/m^3 could be maintained.

Bacteria and Medium

The BTF was inoculated with a biomass suspension of *Hyphomicrobium* sp. GJ21 cultivated in shake flasks. The nutrient stream to the BTF was based on tap water and contained 5.25 kg/m^3 $(NH_4)_2SO_4$, 0.44 kg/m^3 $K_2HPO_4 \cdot 7H_2O$, and 1.75 g/m^3 $FeSO_4$. To maintain the NaCl concentration at the desired level of 150 m*M*, the flow rate to the drain was manually adjusted using a peristaltic pump (603V, Watson and Marlow B.V., Rotterdam, The Netherlands).

Gas and Liquid Phase Analysis

DCM and CO_2 gas phase concentrations were determined with a chromatograph (CP9001, Chrompack Nederland B.V., Bergen op Zoom, The Netherlands) equipped with a 6 ft. × 1/8 in. Hayesep N, 80–100 mesh column. For the DCM and CO_2 analysis, a FID and TCD detector were used, respectively. Helium was used as the carrier gas. The temperature of the column was maintained at 130°C, whereas the temperature of the injector and detector were set at 220°C. Chloroform was measured on a chromatograph (4300, Carlo Erba Strumentazione, Milan, Italy) equipped with a 1 m PEG column and FID detector, with nitrogen as the carrier gas. The temperature of the injector, oven and detector were 120, 110, and 120 °C, respectively. The liquid phase DCM and CO_2 concentrations were determined by the head-space method described by Diks et al. (1994).

Dry Biomass Distribution

The distribution of the dry biomass over the column was obtained by rinsing the column with tap water for 4 h. The whole column was subsequently dried using ambient air, until the weight of the column stabilised. Following this, all packing elements, of which the individual clean weights were known, were weighed separately.

Volumetric Mass Transfer Coefficient

The volumetric mass transfer coefficient of the grown packing was measured using chloroform as an inert tracer compound. The BTF was operated as an once-through cocurrent absorption column and fresh tap water was pumped from a vessel into the BTF. The entering gas stream was enriched with chloroform, which was transferred to the liquid phase in the column. No water was recycled and no substrate was added to the water beforehand. The volumetric mass transfer coefficient was calculated from the decrease of the gas phase concentration along the column.

Numerical Methods

The set of partial differential equations (Eq. (9)) obtained for the reactants and species involved was solved assuming quasi steady-state concentration profiles in the biofilm. This means that local substrate concentrations are assumed to change only at a time scale that is characteristic for the expansion of the biofilm, which is reflected in Eq. (9) (Wanner and Gujer, 1986; Alonso et al., 1997, Kissel et al., 1984). The quasi steady-state concentration profiles in the biofilm were solved using a finite volume method. First, the biofilm concentration profiles were solved using an imposed pH profile to correct for the pH effect on the DCM rate of reaction. Second, a new pH profile was calculated from the Cl^- and total carbonate concentration profiles obtained in the first calculation using Eq. (5). This procedure was repeated until the pH and concentration profiles reached convergence. A similar method was used to obtain the values of u_L at each time step. The liquid and gas phase mass balance equations in the axial direction along the column height were solved simultaneously using an explicit Euler method together with multiple shooting. Calculations started from the top of the column downwards assuming an estimated value of the liquid phase DCM concentration at the top. With the aid of the transversal concentration gradients at the biofilm–water interface obtained from the biofilm calculations, the axial liquid and gas phase concentrations were calculated. A Newton method was used to obtain a new estimate for the liquid phase DCM concentration at the top of the column. After the concentration profiles had reached convergence, a time step was taken and the new biofilm compositions and thicknesses along the column were calculated based on the average growth rate and biofilm composition at the previous time step.

RESULTS

Monitored Parameters

The BTF was operated in a co-current flow mode and with continuous water recycling. It has been claimed that an intermittent water supply may enhance BTF's performance for poorly water soluble compounds like ethene by decreasing the gas-to-biofilm mass transfer resistance (de Heyder et al., 1994; Ockeloen et al., 1992). However, in this study, it was found that cutting off the liquid supply resulted in a 40% decrease of the degree of conversion within six residence times of the gas phase (6 min). This is very likely due to a rapid acidification of the biofilm and its covering liquid film. Table II shows the standard conditions during operation.

The DCM elimination capacity (EC) and the overall rate of CO_2 production in the system (R_{CO2}) were determined daily from the difference between the inlet and outlet DCM and CO_2 concentrations. The maximum elimination capacity (EC^{max}) was determined by increasing the inlet DCM concentration (C_{go}) step by step, until a maximum conversion rate was reached. The obtained graph of the EC versus the C_{go} is called a performance curve. Previous studies give more details on the theoretical and experimental background of this procedure (Diks and Ottengraf, 1991).

To characterise and quantify the biomass and liquid hold-up development on the packing, a distinction was made between the total, static, and dynamic hold-up. The total hold-up G_{tot} is composed of the liquid film flowing on the packing and the total mass of the stationary wet biofilm. This value was determined from the mass of the column under normal operating conditions from which the mass of the empty, dry packed column was subtracted. The static hold-up G_{stat} and dynamic hold-up G_{dyn} were obtained by cutting off the water supply to the BTF and measuring its decrease in mass during drainage. G_{stat} is the mass that remains upon the packing after drainage, and G_{dyn} is the water that has drained from the packing. The hold-ups are difficult to quantify due to the substantial amount of water leaving the biofilm during drainage. Here, G_{tot}, G_{stat}, and G_{dyn} are defined according to the method illustrated in Fig. 3.

Table II. Biotrickling filter conditions during standard operation.

DCM inlet concentration	2	(g/m^3)
pH	7.8–8	
Temperature	20–22	(°C)
NaCl concentration	150	(m*M*)
Liquid hold-up in recycle	About 15	(dm^3)
Reactor volume	332	(dm^3)
Drain	About 2.7	(dm^3/h)
Superficial liquid velocity	7.3	(m/h)
Superficial gas velocity	163	(m/h)

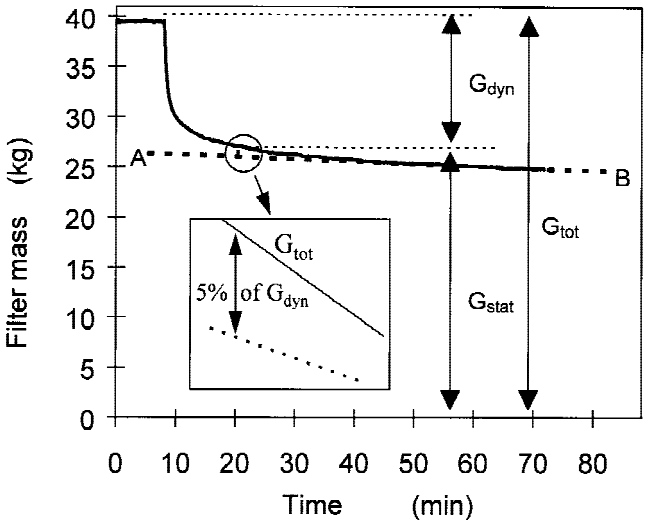

Figure 3. Definition of the total G_{tot}, static G_{stat}, and dynamic G_{dyn} hold-up from a hold-up curve. A straight line is fitted to the slope of the last part of the hold-up curve. G_{stat} is defined as that point where the difference between the straight line and the hold-up curve is 5% of G_{dyn}. —Experimental hold-up curve; (A--B) Straight line fitted through the experimental hold-up curve.

Hold-Up Development

Figure 4 shows a typical example of the development of the total hold-up G_{tot} on the packing shortly before and after a hold-up experiment had been carried out. After the system was restarted, it usually took about 1 day before the mass accumulation rate had regained its original value, while the EC recovered almost instantaneously. Evidently, water drains from the biofilm during a hold-up measurement. In the days that follow, the biofilm re-absorbs water. Together with the steadily decreasing weight observed when a hold-up curve is measured, this supports the assumption that the

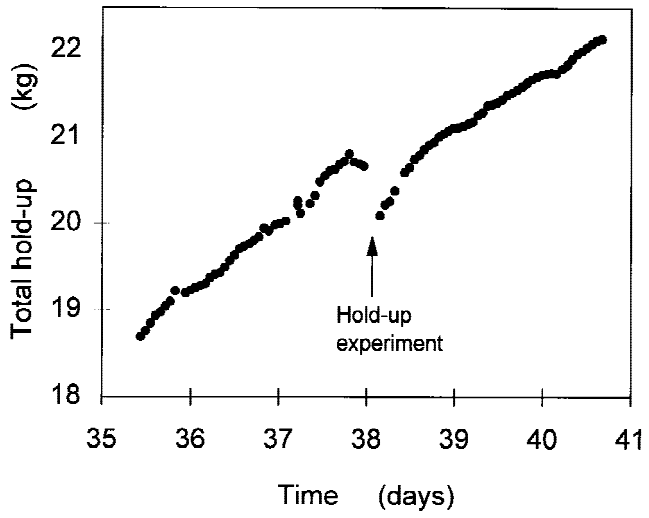

Figure 4. Characteristic total hold-up development before and after a hold-up experiment had been carried out.

biofilm is slightly spongy. A fact that has received much attention in the biofilm literature recently (de Beer et al., 1997; Okabe et al., 1997). The value of G_{dyn} showed a slight increase from about 7 kg after start-up to 10 kg at the end of the experiment.

Except for the start-up period, the development in G_{stat} was linear. A pseudo steady-state biofilm performance, reflected in a linear increase in biofilm thickness or mass, accompanied with a constant EC is well documented in the literature and has been investigated theoretically and experimentally (LaMotta, 1976; Skowlund, 1990; Wanner and Gujer, 1986). A linear G_{stat} accumulation for eight months was also observed by Zuber (1995) in a similar biotrickling filter system.

BTF Performance

The first 3 weeks after inoculation, the BTF was operated with a discontinuous nutrient supply. Fresh nutrient solution was added to the reactor and a few litres of liquid recycle were purged when the sodium chloride concentration reached 300 m*M*. After 23 days, fresh medium was pumped into the reactor, the liquid drain was opened, and from that time on the reactor was operated in a continuous mode of operation. The EC increased rapidly, and within 4 days a pseudo steady state established itself, in which its value was about 1 C mol/($m^3 \cdot h$) (Fig. 5). The EC fluctuated around a mean value and increased slightly during course of time. Biomass wash-out was generally low, an observation consistent with that of Diks et al. (1994). Apparently, the moderate and steady shear forces imposed upon the biofilm by the laminar liquid layer result in a stable biofilm. Larger amounts of biomass were only released in the BTF's recycle flow during cleaning of piping. Biomass wash-out increased over time with peaks of biomass loss probably by the incidental sloughing of larger pieces of old biomass from the grown packing.

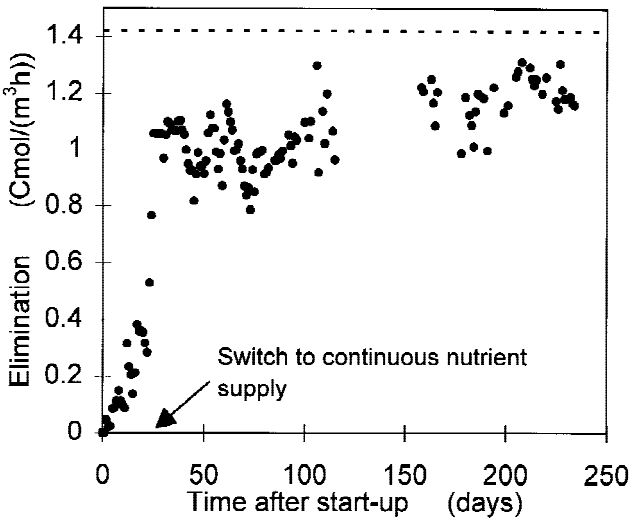

Figure 5. Development of the EC under standard conditions. The horizontal dotted line indicates the applied DCM load.

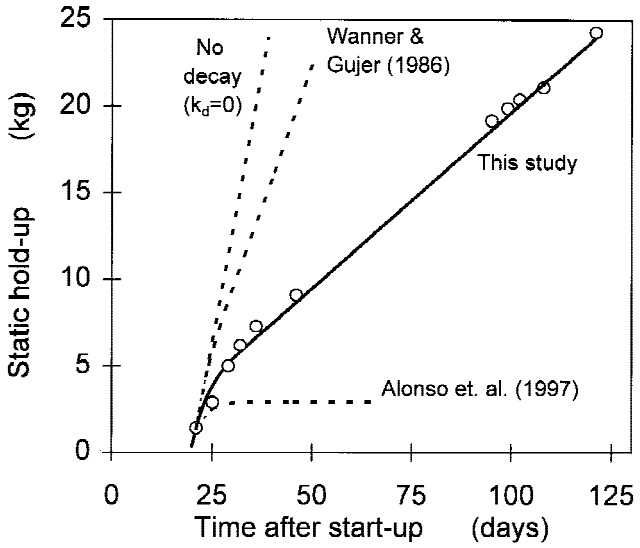

Figure 6. The static hold-up G_{stat} during the course of time (○). Theoretical curves are obtained using the parameter set given in Table III.

Modelling Results

The information contained in the development of G_{stat} and EC can be used to evaluate the modelling results or to obtain information about parameter values. Figure 6 shows the static hold-up G_{stat} development predicted by the model using parameter sets applied in recent biofilm studies, together with the experimental data obtained from the hold-up experiments. The corresponding parameter values are given in Table III. All other parameters used in these simulations are listed in Table I. As already discussed by Skowlund (1990), the assumption of a negligible formation of inerts ($Y_{inert} = 0$) does not lead to a proper description of the data (Alonso et al., 1997; Rittmann and Manem, 1992), because it predicts that the G_{stat} eventually becomes constant with time. Another observation from this figure is that when mineralisation is neglected (no decay), the G_{stat} accumulation predicted by the model is considerably higher than the one that was measured.

There is a considerable deviation among the parameter values reported in Table III. This is probably due to a large natural variety in biofilms and the different ways used to obtain the parameters. Higher decay rates are usually reported for cells in biofilm systems than for cells in suspension. This could well be due to a lack of essential nutrients in the biofilm. Leenen et al. (1997) have shown that the decay rate strongly depends on the concentration of ammonium and oxygen in the medium.

An estimate for the model parameters X, k_d, and Y_{inert} for the present system was made from the EC reached in the system and the G_{stat} accumulation observed. As the DCM degradation rate is directly proportional to the biomass concentration in the biofilm, X (Eqs. (1) and (10)), this variable has the largest influence of all three kinetic parameters. Therefore, in the theoretical model, X was varied until the

Table III. Biofilm kinetic parameters and stoichiometric parameters used in literature. The parameter sets are translated into the specific parameter types applied in this study.

Parameter	k_d (10^{-6} s^{-1})	Y_{inert} (–)	X_{act} (kg/m^3)
Present study	3.2	0.13	75
Alonso et al. (1997)	5.0	0	17
Arcangeli and Arvin (1992)	6.9	0.20	112
Horn and Hempel (1997)	5.8	0.60	28/48[a]
Rittmann and Manem (1992)	0.58	0	13
Wanner and Gujer (1986)	2.3	0.30	4

[a]Autotrophs/inerts.

simulated EC equalled the experimentally measured one. The parameters k_d and Y_{inert} were estimated from the experimentally determined development of the G_{stat} values in time (Fig. 6). Their values were within the range of the values found in the literature.

Model Verification

Carbon Balance

Figure 7 shows the model simulation of the measured overall rate of CO_2 production (R_{CO2}) relative to the EC, together with the experimental data. It gives the degree of carbon fixation in the system. After a first sharp increase due to an increase in EC, it took approximately 14 days before R_{CO2}/EC reached its maximum. According to the model predictions, a net carbon fixation of about 6% of the EC is responsible for the observed G_{stat} accumulation in the pseudo steady state. This value corresponds with the average of the experimental data shown in Fig. 7.

The carbon balance shows that the DCM degrading system is close to the point where no net carbon fixation occurs, namely, a situation referred to as a "biological equilibrium" by Diks et al. (1994). R_{CO2} is about 0.94 times the molar EC. Formaldehyde is the growth precursor when DCM is used as a substrate. The theoretical yield coefficient for growth on formaldehyde is 0.47, and on the basis of this yield a R_{CO2}/EC value of 0.53 is expected (Roels, 1983). The CO_2 produced in excess of this value is therefore due to mineralisation of biomass by processes like biomass decay. Since this fraction is relatively high, it is shown that biomass mineralisation is indeed a relatively important mechanism in the system.

Axial Distribution of Biomass

Figure 8 shows the experimentally measured and theoretically calculated axial distribution of the dry biomass. It can be concluded that an asymmetrical biomass distribution is obtained and that the model predictions agree rather well with the experimental data. The higher biomass concentration in the top section of the column in the experiments can be explained by the locally enhanced mass transfer due to the presence of the liquid distributor.

Reaction Inhibition by Acid Production

Due to the production of hydrochloric acid during the oxidation of DCM, the pH decreases downstream of the filter bed and inside the biofilm. This causes a decrease in the intrinsic rate of reaction. The decrease of pH along the height of the column depends upon the EC, the applied buffer concentrations and the liquid phase residence time. It has been shown for nitrifying biofilms that pH gradients affect the conversion rate in a biofilm (Szwerinski et al., 1986). Reaction inhibition in such biofilms may already occur before the pH in the bulk liquid drops significantly.

The experimental performance curve determined at the

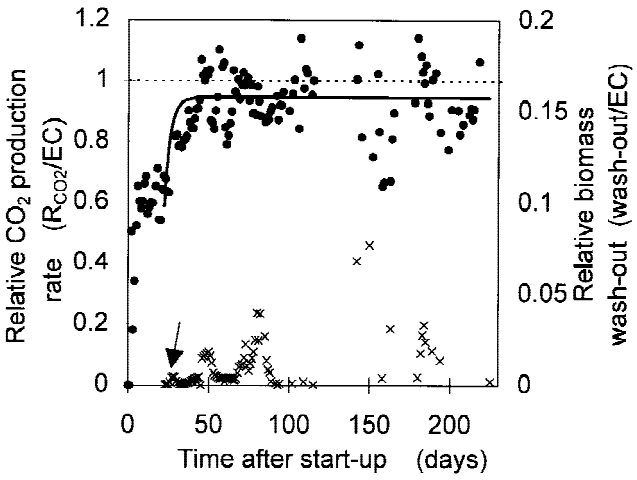

Figure 7. Carbon balance of the BTF. R_{CO2} and the biomass wash-out are given relative to the EC. (●) R_{CO2}; (×) biomass wash-out; (—) model simulation of the R_{CO2}. The arrow indicates the switch to a continuous nutrient supply.

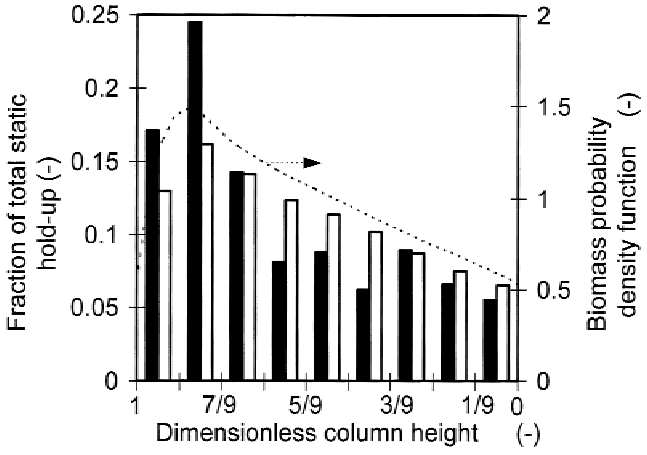

Figure 8. Measured and predicted dry weight distribution along the filter bed. Black bars are measurements; white bars are model predictions. The dotted line is the model prediction for the biomass distribution function. The measurement was carried out at the end of a previous run with the BTF, in which the same standard conditions were applied.

standard buffer concentration was simulated using the model parameters given in Table I. Experimental and theoretical results are shown in Fig. 9. The model describes the experimentally found EC^{max} curves fairly well. There was a marked and reproducible difference between the performance curve measured with and without a phosphate buffer in the liquid, illustrating the inhibition of the reaction by the produced acid. At elevated gas inlet concentrations, the addition of a buffer solution increased the EC instantaneously, which coincided with an increase in pH at the base of the column from about 5.2 to 6.4. From Fig. 9 it can also be concluded that at lower gas phase concentrations ($C_{go} < 2$ g DCM/m^3) there is no appreciable difference in performance between the rich buffer solution and tap water under the conditions applied. Model simulations showed that this is the result of the buffering capacity of bicarbonate ions produced in the bio-oxidation. The model simulations in Fig. 9 show that without any buffering capacity of the water recycle, the expected drop in performance is large.

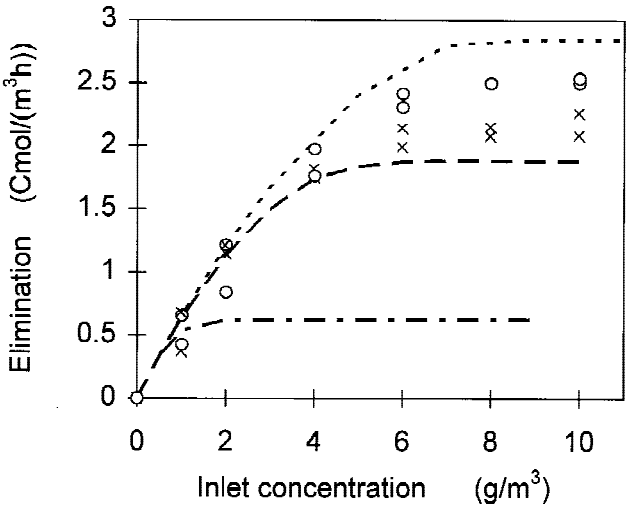

Figure 9. Performance curves measured at two different total phosphate buffer concentrations, together with the corresponding model simulations. The influence of the buffer concentrations is illustrated by the predicted performance curve without any buffers present. (○) Standard nutrient concentration; (×) tap water. Dotted lines are model simulations: (---) standard nutrient concentration; (– –) tap water, containing $C_t = 1.5$ mM and $P_t = 0$; (– · –) no buffers.

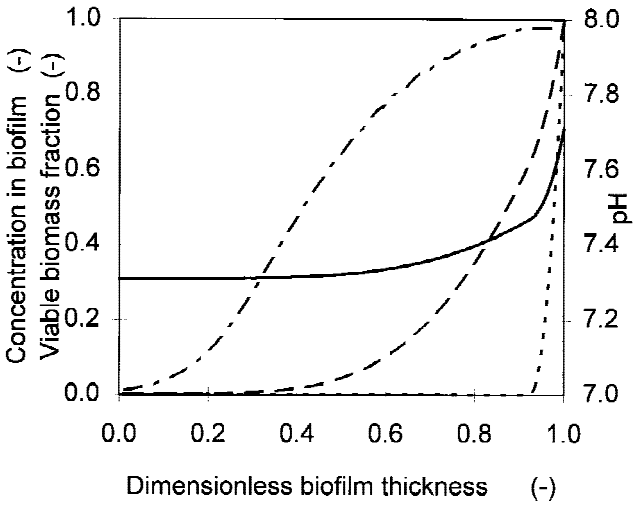

Figure 10. Dimensionless biofilm concentration profiles predicted by the model at $\sigma = 0.93$ (close to the top of the column): (---) DCM; (– –) oxygen; (—) pH; (– · –) viable biomass.

Transversal Biofilm Concentration Profiles

Under standard conditions, the DCM rate of conversion is limited by the diffusion of DCM, not by oxygen. Figure 10 shows a typical example of the model predictions for the transversal concentration profiles and the active biofilm fraction in the biofilm under standard conditions. The DCM penetration depth that determines the active biofilm volume is much lower than the thickness of the layer in which the main part of the biomass is viable. Furthermore, it is clear that anaerobic zones are present in deeper levels of the biofilm during standard conditions. They do not originate from the bio-oxidation of DCM, however, but rather from the mineralisation of biomass. Dark brown/black areas on the grown packing were indeed observed in the column. They are an indication of anaerobic zones in the system. The slight decrease in pH in deeper levels of the biofilm is the result of the production of CO_2 in the mineralisation process.

Increasing the DCM concentration in the gas phase increases the DCM penetration depth and therefore the flux of DCM through the biofilm–water interface. The model predicts that oxygen transfer becomes rate limiting for the DCM degradation at inlet concentrations above about 7 g/m^3.

An important practical consequence follows from the fact that viable biomass is present throughout a relatively large depth of the biofilm (Fig. 10). From batch degradation experiments, it is known that the DCM degradation resumes within a short period after the biomass has been starved for several days. These two observations indicate that after a stepwise increase in the gas phase concentration, adaptation takes place relatively quickly. Viable biomass is still present in deeper levels of the biofilm and these cells will be reactivated whenever the DCM concentration increases. This is indeed what is found in practice. Figure 11 shows the experimental and simulated response of the EC to a stepwise increase of the gas inlet concentration from 2 to 6 g DCM/m^3. Within a day, the EC had stabilised at an 88% higher value, a value that also results from model simulations.

Clogging Time and Maximum Carbon Load

Clogging of BTFs with excessive biomass is often observed at higher carbon loads. In our laboratory, clogging of BTFs was observed on a wide range of time scales, from a period of several weeks to over six months, depending on the type of system investigated and the carbon load applied. Never-

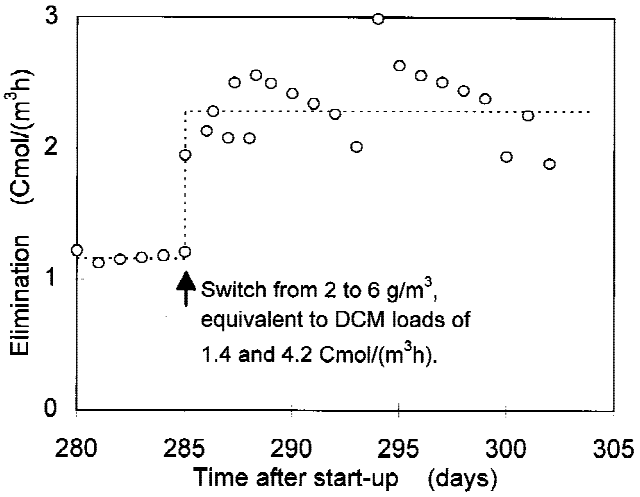

Figure 11. Measured and simulated response of the EC to a stepwise increase in the DCM inlet concentration from 2 to 6 g/m^3.

theless, BTFs eliminating DCM from waste gases could be operated for over 4 years without any clogging.

Clogging is a complex phenomenon determined by such diverse factors as the biological and physical characteristics of the compounds involved, e.g., their microbial degradation rates and Henry coefficients, the mechanical strength and morphology of the formed biofilm—especially its density—and the structural characteristics of the packing material. Regarding the biofilm structure, for example, it is known that growth on certain substrates, especially aromatic compounds like toluene and styrene, favours the development of fungi. They yield a much lower average density of the formed biomass and therefore a higher packing volume is occupied in a shorter time. The large diversity between different microbial systems makes it difficult to generalise results.

The mass accumulation rate in a BTF determines at what rate the packing becomes filled up with biomass. In the pseudo steady state the accumulation of the static hold-up is linear (Fig. 6). If a constant wet biofilm density is assumed, the decrease in void volume in time will be linear, too. For a given system, the rate of biomass accumulation is mainly determined by the imposed load. Here, it should be stressed that in order to compare loads of different systems, the preferred units are carbon moles (C mol) rather than units based on mass (kg). Due to the low carbon content of substances like DCM and CS_2, their molar loads are generally low. Toluene, for example, will give a molar carbon load of over six times that of DCM, when an equal mass load is imposed. Besides a low average growth rate, this is another reason for the relatively slow mass accumulation rate in the DCM system. Biomass accumulation is fast with methylmethacrylate or toluene as pollutants. As a result, biomass has to be removed frequently from the packing, e.g., by back-washing or addition of chemicals (Alonso, 1997; Diks, 1992; Weber, 1995).

From Figure 8, it is clear that the biomass is not uniformly distributed along the column at all. The top section of a co-currently operated BTF will therefore plug earlier than its lower sections, nearly twice as fast in this study. Figure 12 illustrates that maldistribution of the biomass becomes more pronounced when the wetted packing area increases at a constant voidage.

Modelling may help to estimate the clogging time of a filter at various carbon loads. The relevant criterion for clogging is the pressure drop along the column. At gas flow rates usually applied in BTFs (100–600 m/h), biological waste gas treatment systems equipped with a fan can be operated up to a pressure drop of about 800 Pa/m.

Pressure drop data for the flow of gas through beds of solids are not readily correlated, however, because of the variety of packing materials and their arrangement. If the biomass development on the packing is uniformly distributed throughout the bed, the rise in pressure drop can be estimated from correlations given in literature, e.g., by Ergun or Leva (Perry and Chilton, 1973). These correlations show that the pressure drop is inversely proportional to the fractional void volume of the packed bed to the power of three. Consequently, a steep rise in the pressure drop in different packed bed systems for waste gas treatment systems is encountered at critical voidage ε_c of 0.2–0.4. Diks (1992) observed the beginning of clogging at a critical voidage of 0.38 in a previous run of the BTF with the same arranged packing material as used in this study, with acetone as a pollutant and a gas flow rate of 200 m/h. Figure 13 shows the characteristic development of the pressure drop measured for dumped 1 inch saddles. The figure illustrates that clogging starts rather suddenly after a period of undisturbed operation. The clogging data can be approxi-

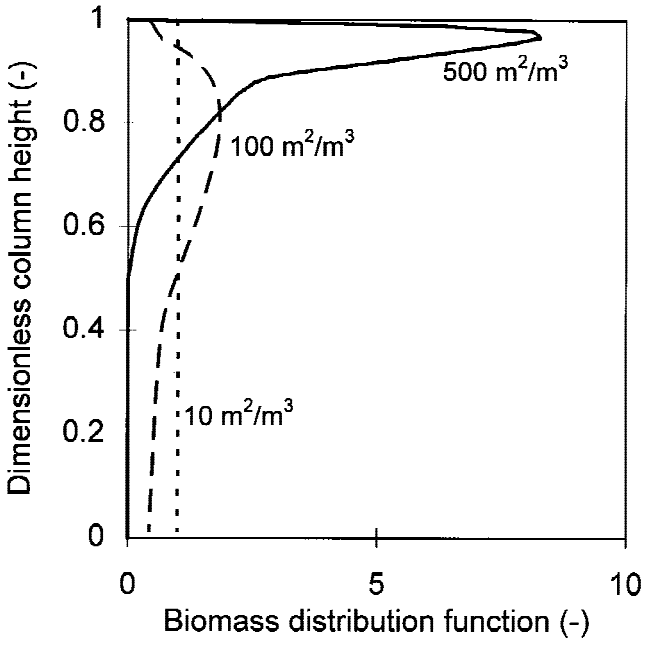

Figure 12. Shift in the biomass distribution along the column when the specific wetted packing area is increased: (—) specific wetted area 500 m^2/m^3; (– –) 100 m^2/m^3; (· · ·) 10 m^2/m^3.

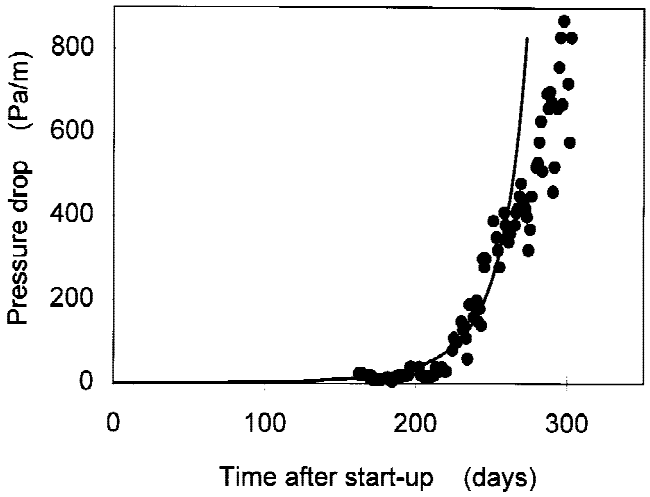

Figure 13. Characteristic pressure drop development. Data were fitted using the Leva correlation (Perry and Chilton, 1973) and the assumption of a linearly decreasing voidage. At day 220 the voidage reaches the critical voidage of 0.3. (1″ supertorus saddles, $\varepsilon_u = 0.93$, EC = 1.0 C mol/($m^3 \cdot h$), inlet concentration DCM = 0.4 g/m^3, inlet concentration MMA = 0.05 g/m^3, $v_g = 200$ m/h).

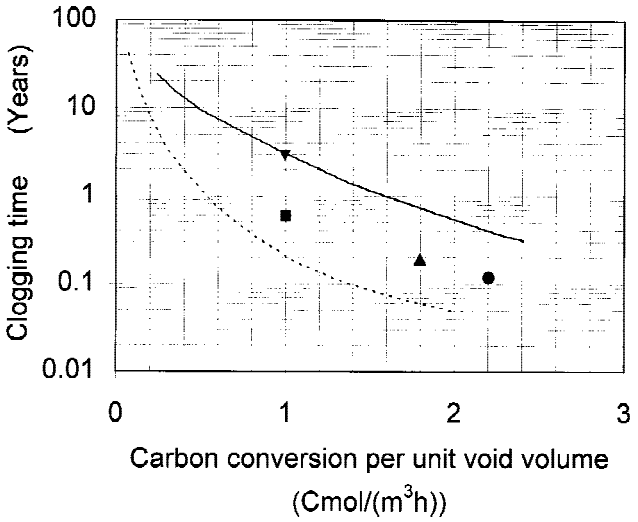

Figure 14. Model simulation of the characteristic clogging time τ_{clog} of the BTF at standard conditions as a function of the carbon conversion per unit void packing volume: (—) DCM; (· · ·) toluene. Physical and biological parameters for toluene have been taken from Alonso et al. (1997). The critical voidage ε_c was set at 0.3. (●) Acetone, cross flow packing, $\varepsilon_u = 0.97$, Diks (1992); (▲) toluene, Novalox torus saddles, $\varepsilon_u = 0.71$, Diks (1992); (■) DCM/methylmethacrylate, supertorus saddles, $\varepsilon_u = 0.91$ (Okkerse et al., 1998); (▼) this study.

mated very well using a pressure drop correlation from literature and the assumption of a linearly decreasing fractional void volume during the course of time.

A rough estimate of the characteristic time involved in clogging processes can be made by calculation of the time needed to reach the critical packed bed voidage ε_c. This characteristic time can be estimated from the void packing volume to-be-filled-up and the measured or simulated rate of mass accumulation in the system

$$\tau_{clog} = \rho_b \cdot V_r \cdot (\varepsilon_u - \varepsilon_c)/\dot{G}_{tot} \qquad (16)$$

in which ε_u is the voidage of the ungrown packed bed. Figure 14 shows the simulated dependence of the clogging time on the carbon conversion rate for the investigated system loaded with DCM, and with toluene. For comparison also some experimental clogging data are included in the figure. The figure shows that there is a significant difference between the two systems, which is mainly due to the difference in biofilm density. This can be considered as the characteristic difference between a slow growing biofilm with a high density (e.g., growth on DCM), and a rapidly growing biofilm with a low density (e.g., growth on toluene).

For design purposes, process engineers are interested in a simple rule of thumb for the maximum allowable carbon load that can safely be applied. Within the light of the foregoing analysis, it is advocated to use the rate of carbon conversion per unit void packing volume (CCV) when loads of different systems are compared. Figure 14 shows that above a CCV of 0.5–1.6 C mol/($m^3 \cdot h$) the clogging time becomes a matter of months, rather than years. Higher loads should not be applied without proper counter-measures to remove excessive biomass from the filter. Figure 14 shows also that the clogging time increases stronger than exponentially with a decreasing VOC inlet concentration. At the low CCV values usually encountered in odour control, a stable operation is therefore guaranteed.

Evidently, the maximum CCV deduced here is a conservative estimate. During the course of time, processes that reduce the amount of immobilised biomass on the packing increase in importance, like for example an enhanced biomass wash-out due to sloughing of ageing biomass as observed in this study. Periods of starvation and disturbances in operating conditions add to these biomass removal processes. A nutrient limited and dry environment—as found in biofilters—will increase the maximum CCV that can be applied, as these conditions increase the biomass decay rate (Leenen et al., 1997) and might decrease the yield factor.

CONCLUSIONS

A dynamic BTF model was presented that adequately describes the degradation of a volatile acidifying pollutant in a biotrickling filter, as well as the resulting mass accumulation in the system and mass distribution along the column. It takes into account reaction inhibition by the production of acid, and a distinction is made between active and inactive biomass. The model is suitable for optimisation and design purposes and provides insight into the dominating biological and physical BTF mechanisms.

Weighing of the experimental filter unit has proven to be a powerful tool to gain information about the development of the different mass hold-ups on the packing of the BTF. It gives the development of the wet biomass on the packing as

extra information that can be used to evaluate modelling results. In contrast to indirect methods like the study of the carbon balance, weighing of the filter has the advantage of being both accurate and direct. As a result, long-term studies to evaluate filter clogging can be avoided.

A comparison to other BTF systems demonstrates that it is difficult to generalise results, as there is a large natural variety in biofilm systems. The modelling carried out in this work shows that a basic distinction should be made between slowly growing, dense biofilms and rapidly growing, low-density biofilms. Furthermore, a comparison of loading rates should always be made on a molar, instead of on a mass basis.

The time scale involved in the clogging process of packed beds was estimated from the results of the model simulations. They showed that above a carbon conversion per unit void packing volume (CCV) of 0.5–1.6 C mol/($m^3 \cdot h$) the characteristic time for clogging becomes a matter of months, rather than years and proper countermeasures to prevent or minimise clogging phenomena may be necessary. The exact value of the maximum load depends on the characteristics of the reactor system and the properties of the formed biomass.

The modelling efforts have shown that it is necessary to include biomass mineralisation in the model in order to accurately describe the mass accumulation in the system. It was also shown that addition of a phosphate buffer is not necessary at DCM inlet concentrations lower than 2 g/m^3 due to the relatively high buffering capacity of the bicarbonate ions in the liquid recycle.

The authors thank the graduate students J. Dekker, M. Willemsen, and E. Swaans for their help in obtaining and evaluating the data presented in this paper.

NOMENCLATURE

Γ_i	flux of compound *i* in the biofilm (kg/(m^2s))
$\Gamma_{i,L}$	flux of compound *i* at the biofilm–water interface (kg/(m^2s))
ε	fractional void packing volume or voidage (–)
ε_c	voidage at which a critical pressure drop is reached (–)
ε_u	voidage of the ungrown packed bed (–)
ζ	dimensionless biofilm length coordinate, *x*/*L* (–)
μ_{max}	maximum specific growth rate (1/s)
$\overline{\mu}$	average local growth rate (1/s)
μ_{act}	specific growth rate of the active, DCM degrading population (1/s)
μ_{inert}	specific growth rate of the inerts (1/s)
τ_{clog}	clogging time (time unit)
υ_i	stoichiometric coefficient of compound *i* liberated in the bio-oxidation (–)
$\upsilon_{i,d}$	stoichiometric coefficient of compound *i* liberated in biomass decay (–)
ρ_b	biofilm density (kg/m^3)
σ	dimensionless column height (–)
A	fitting parameter in Eq. (2) (–)
a_w	wetted packing area (1/m)
B	fitting parameter in Eq. (2) (–)
$c_{L,i}$	bulk liquid concentration of compound *i* (kg/m^3)
$c_{G,i}$	gas phase concentration of compound *i* (kg/m^3)
C_{go}	DCM inlet concentration (kg/m^3)
C_t	total carbonate concentrations (mol/m^3)
D_i	diffusion coefficient of the specific substrate (m^2/s)
EC	rate of substrate elimination in the system (C mol/($m^3 \cdot h$))
EC^{max}	maximum rate of substrate elimination in the system (C mol/($m^3 \cdot h$))
f_{act}	active biomass volume fraction (–)
$f_{act,o}$	initial active biomass volume fraction across the biofilm (–)
f_{inert}	volume fraction of inert mass (–)
F_{pH}	function that describes the pH dependence of the DCM degradation (–)
G_{dyn}	dynamic hold-up, defined in Fig. 3 (kg)
G_{stat}	static hold-up, defined in Fig. 3 (kg)
G_{tot}	total hold-up, defined in Fig. 3 (kg)
$\dot{G}_{tot}$	total hold-up accumulation rate (kg/s)
H	Height of the BTF packing (m)
K_1	carbon dioxide to bicarbonate dissociation constant (mol/m^3)
K_2	mono- to bihydrogenphosphate dissociation constant (mol/m^3)
K_i	Monod constant of compound *i* (kg/m^3)
k_d	biomass decay or mineralisation constant (1/s)
$k_{og}a_w$	volumetric mass transfer coefficient (1/s)
L_o	initial biofilm thickness (m)
L	biofilm thickness (m)
m	gas–liquid distribution coefficient (–)
M_i	molar mass of compound *i* (kg/mol)
P_t	total phosphate concentration (mol/m^3)
R_{CO2}	overall rate of CO_2 production (mol/($m^3 \cdot h$))
r_i	intrinsic rate of reaction of compound *i* in the biofilm (kg/($m^3 \cdot s$))
r_d	biomass mineralisation rate (kg/$m^3 \cdot s$)
S_i	biofilm concentration of compound *i* (kg/m^3)
u	biofilm expansion rate relative to the film/support interface (m/s)
u_L	biofilm–water interface expansion rate (m/s)
V_r	BTF volume (m^3)
v_l	superficial liquid velocity (m/s)
v_g	superficial gas velocity (m/s)
x	length coordinate in the biofilm (m)
X	total biomass concentration (kg/m^3)
X_{act}	active biomass concentration (kg/m^3)
X_{inert}	concentration of inerts (kg/m^3)
Y_{DCM}	yield of biomass on DCM (–)
Y_{inert}	yield of inerts on biomass (–)
z	length coordinate along the column (m)

References

Alonso C, Suidan MT, Sorial GA, Smith FL, Biswas P, Smith PJ, Brenner RC. 1997. Gas treatment in trickle-bed biofilters: how much biomass is enough? Biotechnol Bioeng 54:583–594.

Arcangeli JP, Arvin E. 1992. Modeling of toluene biodegradation and biofilm growth in a fixed biofilm growth in a fixed biofilm reactor. Water Sci Technol 29:617–626.

Bryers JD, Mason CA. 1987. Biopolymer particulate turnover in biological waste treatment systems: A review. Bioprocess Eng 2:95–109.

de Beer D, Stoodley P, Lewandowski Z. 1997. Measurements of local diffusion coefficients in biofilms by microinjection and confocal microscopy. Biotechnol Bioeng. 53(2):152–158.

de Heyder B, Overmeire A, Van Langenhove H,Verstraete W. 1994. Ethene removal from a synthetic waste gas using a dry biobed. Biotechnol Bioeng 44:642–648.

Deshusses MA, Hamer G, Dunn IJ. 1995. Behavior of biofilters for waste air biotreatment. Experimental evaluation of a dynamic model. Environ Sci Technol 29:1059–1068.

Diks RMM. 1992. The removal of dichloromethane from waste gases in a biological trickling filter. Thesis, Eindhoven University of Technology, Eindhoven, The Netherlands.

Diks RMM, Ottengraf SPP. 1991. Verification studies of a simplified model for the removal of dichlomethane from waste gases using a

biological trickling filter. Parts I and II. Bioprocess Eng 6:93–99, 131–140.

Diks RMM, Ottengraf SPP, Vrijland S. 1994. The existence of a biological equilibrium in a trickling filter for waste gas purification. Biotechnol Bioeng 44:1279–1287.

Fan LS, Leyva-Ramos R, Wisecarver KD, Zehner BJ. 1990. Diffusion of phenol through a biofilm grown on activated carbon particles in a draft-tube three-phase fluidized-bed bioreactor. Biotechnol Bioeng 23: 279–286.

Hekmat D, Vortmeyer D. 1994. Modelling of biodegradation processes in trickle-bed bioreactors. Chem Eng Sci 49:4327–4345.

Horn H, Hempel DC. 1997. Substrate utilization and mass transfer in an autotropic biofilm system: Experimental results and numerical simulations. Biotechnol Bioeng 53(4):363–371

Janssen LPBM, Warmoeskerken MMCG. 1979. Transport phenomena data companion. Delft, The Netherlands: DUM B.V.

Kirchner K, Wagner S, Rehm HJ. 1996. Removal of organic air pollutants from exhaust gases in the trickle-bed bioreactor. Effect of oxygen. Appl Microbiol Biotechnol 45:415–419.

Kissel JC, McCarty PL, Street RL. 1984. Numerical simulation of mixed-culture biofilm. J Environ Eng 10:393–411.

LaMotta EJ. 1976. Internal diffusion and reaction in biological films. Environ Sci Technol 10(8):765–769.

Leenen EJTM, Boogert AA, van Lammeren AAM, Tramper J, Wijffels RH. 1997. Dynamics of artificially immobilized *Nitrosomonas europaea:* Effect of biomass decay. Biotechnol Bioeng 55:631–641.

Liou JK, Rousseau I. 1986. Mathematical model for internal pH control in immobilized enzyme particles. Biotechnol Bioeng 28:1582–1589.

Mehrbach C, Cuberson CH, Hawley JE, Pytkowicz RM. 1973. Measurement of the apparent dissociation constant of carbonic acid in seawater at atmospheric pressure. Limnol Oceanogr 18(6):897–907.

Ockeloen HF, Overcamp TJ, Grady CDL. 1992. A biological fixed film simulation model for the removal of volatile organic pollutants. In: Proceedings of the 85th Annual Meeting of the AMWA, Kansas City, MO.

Okabe S, Hiratia K, Ozawa Y, Watanabe Y. 1996. Spatial microbial distributions of nitrifyers and heterotrophs in mixed-population biofilms. Biotechnol Bioeng 50:24–35.

Okabe S, Yasuda T, Watanabe Y. 1997. Uptake and release of inert fluorescence particles by mixed population biofilm. Biotechnol Bioeng 53(5):459–469.

Okkerse WJH, Ottengraf SPP. 1997. Change in wetting properties of a structured PVC packing due to biofilm growth. In: Proceedings of the International Symposium on Environmental Biotechnology, Oostende, April 21–23, Belgium. p 231–235.

Okkerse WJH, Ottengraf SPP, Diks RMM, Osinga-Kuipers B, Jacobs P. 1999. Long term performance of biotrickling filters removing a mixture of volatile organic compounds from an artificial waste gas: dichloromethane and methylmethacrylate. Bioprocess Eng. 20:49–57.

Ottengraf SPP. 1986. Exhaust gas purification. In: Rehm HJ, Reed G., editors. Biotechnology. Weinheim: VCH Verlagsgesellschaft. p 425–452.

Pedersen AR, Arvin E. 1997. Effect of biofilm growth on the gas–liquid mass transfer in a trickling filter for waste gas treatment. Water Res 31(8):1963–1968.

Perry PX, Chilton FF, editors. 1997. Chemical engineers handbook. 5th ed. New York: McGraw-Hill.

Rittmann BE, Manem JA. 1992. Development and experimental evaluation of a steady-state, multispecies biofilm model. Biotechnol Bioeng 39: 914–922.

Roels JA. 1983. Energetics and kinetics in biotechnology. Amsterdam: Elseviers Biomedical.

Shareefdeen ZS, Baltzis BC, Oh YS, Bartha R. 1993. Biofiltration of methanol vapor. Biotechnol Bioeng 41:512–524.

Shareefdeen Z, Baltzis BC. 1995. Biofiltration of toluene vapor under steady-state and transient conditions: Theory and experimental results. Chem Eng Sci 49(24a):4347–4360.

Sharma MM, Danckwerts PV. 1970. Chemical methods of measuring interfacial area and mass transfer coefficients in two-fluid systems. Br Chem Eng 15(4):528.

Skowlund CT. 1990. Effect of biofilm growth on steady-state biofilm models. Biotechnol Bioeng 35:502–510.

Szwerinski H, Arvin E, Harremoes P. 1986. pH decrease in nitrifying biofilms. Water Res 20(8):971–976.

Wanner O, Gujer W. 1986. A multispecies biofilm model. Biotechnol Bioeng 28:314–328.

Weber F. 1995. Toluene: biological waste gas treatment, toxicity and adaptation. Thesis. Wageningen Agricultural University. Wageningen, The Netherlands.

Wik T, Breitholtz C. 1996. Steady-state solution of a two species biofilm problem. Biotechnol Bioeng 50:675–686.

Zarook SM, Shaikh AA, Ansar Z. 1997. Development, experimental validation and dynamic analysis of a general biofilter model. Chem Eng Sci 52(5):759–773.

Zuber L. 1995. Trickling filter and three-phase airlift bioreactor for the removal of dichloromethane from air. PhD thesis. Swiss Federal Institute of Technology. Zurich. Switzerland.